Resource

Developmental Cell

An Integrated Transcriptome Atlas of Embryonic Hair Follicle Progenitors, Their Niche, and the Developing Skin

Graphical Abstract

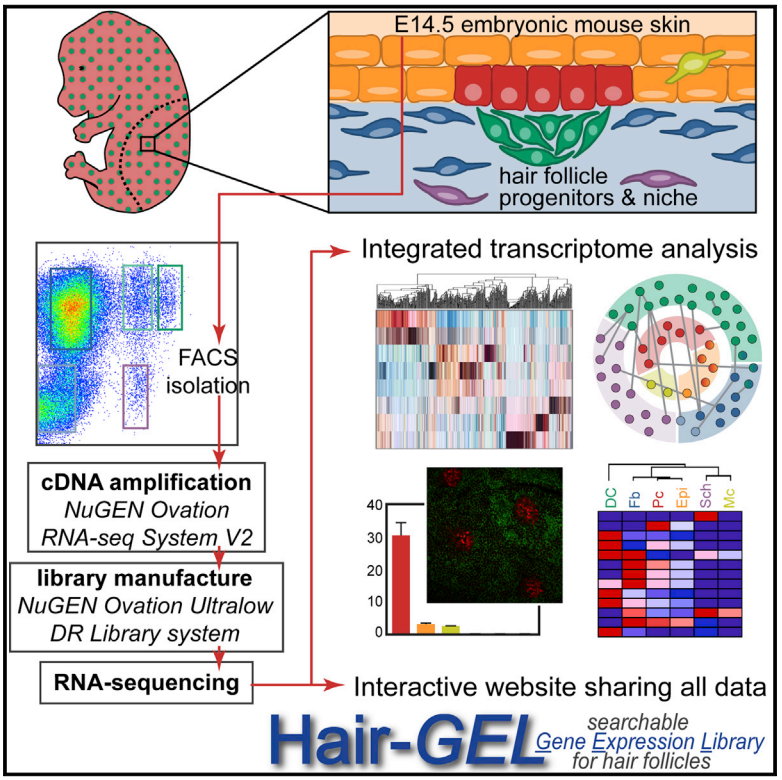

Authors

Rachel Sennett, Zichen Wang, Amélie Rezza, ..., Carlos Clavel, Avi Ma'ayan, Michael Rendl

Correspondence

michael.rendl@mssm.edu

In Brief

The gamut of molecular messengers exchanged during the epithelial-mesenchymal interactions driving hair follicle morphogenesis are unknown. Sennett et al. isolate hair follicle progenitor and niche cells alongside all other cells from embryonic skin and use RNA sequencing to define gene expression signatures of distinct cell types within a heterogeneous tissue.

Highlights

- Embryonic skin is made up of heterogeneous cell types during hair follicle formation
- A comprehensive transcriptomic analysis of developing skin is presented
- Hair follicle progenitor/niche cells express unique genes imparting functionality

Accession Numbers

GSE70288

Sennett et al., 2015, Developmental Cell *34*, 577–591
September 14, 2015
http://dx.doi.org/10.1016/j.devcel.2015.06.023

CellPress

Developmental Cell
Resource

An Integrated Transcriptome Atlas of Embryonic Hair Follicle Progenitors, Their Niche, and the Developing Skin

Rachel Sennett,[1,2,4] Zichen Wang,[1,4,5] Amélie Rezza,[1,2] Laura Grisanti,[1,2] Nataly Roitershtein,[1,2] Cristina Sicchio,[1,2] Ka Wai Mok,[1,2] Nicholas J. Heitman,[1,2,4] Carlos Clavel,[1,2] Avi Ma'ayan,[1,4,5] and Michael Rendl[1,2,3,4,*]
[1]Black Family Stem Cell Institute
[2]Department of Developmental and Regenerative Biology
[3]Department of Dermatology
[4]Graduate School of Biomedical Sciences
[5]Department of Pharmacology and Systems Therapeutics, BD2K-LINCS Data Coordination and Integration Center, Knowledge Management Center for Illuminating the Druggable Genome (KMC-IDG)
Icahn School of Medicine at Mount Sinai, New York, NY 10029, USA
*Correspondence: michael.rendl@mssm.edu
http://dx.doi.org/10.1016/j.devcel.2015.06.023

SUMMARY

Defining the unique molecular features of progenitors and their niche requires a genome-wide, whole-tissue approach with cellular resolution. Here, we co-isolate embryonic hair follicle (HF) placode and dermal condensate cells, precursors of adult HF stem cells and the dermal papilla/sheath niche, along with lineage-related keratinocytes and fibroblasts, Schwann cells, melanocytes, and a population inclusive of all remaining skin cells. With next-generation RNA sequencing, we define gene expression patterns in the context of the entire embryonic skin, and through transcriptome cross-comparisons, we uncover hundreds of enriched genes in cell-type-specific signatures. Axon guidance signaling and many other pathway genes are enriched in multiple signatures, implicating these factors in driving the large-scale cellular rearrangements necessary for HF formation. Finally, we share all data in an interactive, searchable companion website. Our study provides an overarching view of signaling within the entire embryonic skin and captures a molecular snapshot of HF progenitors and their niche.

INTRODUCTION

Hair follicle (HF) regeneration in the adult hair cycle is driven by quiescent and activated stem cells (SCs) in the bulge and hair germ (Greco et al., 2009; Hsu et al., 2011) and coordinated by signal exchange from the dermal papilla (DP) niche (Rezza et al., 2014; Sennett and Rendl, 2012). While these adult SCs and niche cells have been isolated and characterized at a genome-wide level (Blanpain et al., 2004; Greco et al., 2009; Lien et al., 2011; Morris et al., 2004; Rendl et al., 2005; Tumbar et al., 2004), a comprehensive and integrated analysis of the unique molecular features that define their embryonic precursors in nascent HFs, within the context of the entire developing skin, has been lacking. Identifying the internal and external signaling mechanisms during HF morphogenesis is key to understanding the dynamic epithelial-mesenchymal interactions at work during complex tissue development; it also is the first instrumental step in advancing clinical attempts to regulate hair growth and generate fully functional skin grafts including HFs.

HF morphogenesis is initiated during embryonic skin development after secreted epidermal Wnts activate broad dermal Wnt signaling activity (Chen et al., 2012), which, in turn—through unknown downstream signaling—leads to hair placode (Pc) induction in the epidermis and dermal condensate (DC) formation below (Figure 1A) (Millar, 2002; Schneider et al., 2009; Sennett and Rendl, 2012). Genetic fate mapping studies established Pc cells as the earliest progenitors of all epithelial HF cells, including adult SCs in the bulge (Levy et al., 2005), and DC cells as the precursors of DP/dermal sheath niche cells within the mature follicle (Grisanti et al., 2013a). Continued signaling between these progenitor cells is required for downgrowth and formation of mature HFs, but the precise identity and order of all molecular messengers driving this complex process are not yet fully known (Ahn, 2015; Biggs and Mikkola, 2014).

Prior investigations of these events have been narrow in their exclusive focus on only Pc or DC cells. While Pc progenitors are known to generate a handful of signals important for some aspects of hair morphogenesis—for example, *Eda* for maintaining Pcs (Laurikkala et al., 2002; Zhang et al., 2009), *Fgf20* for inciting condensate formation (Huh et al., 2013), and *Shh* for promoting hair downgrowth (Chiang et al., 1999; St-Jacques et al., 1998)—much less is known regarding the dermal response and contribution to this crucial signaling exchange. Wnt signaling in DCs is important for the progression of HF formation (Tsai et al., 2014), and a number of additional factors are distinctly upregulated in condensates compared to non-specialized dermal fibroblasts (Fb) in embryo skin, but, as of present, few have proven required for HF formation (Grisanti et al., 2013a, 2013b; Rezza et al., 2015; Sennett et al., 2014). Importantly, the skin is incredibly heterogeneous by embryonic day (E)14.5, when Pcs and condensates first start to appear, and signaling from multiple sources in the micro- and macroenvironment could be

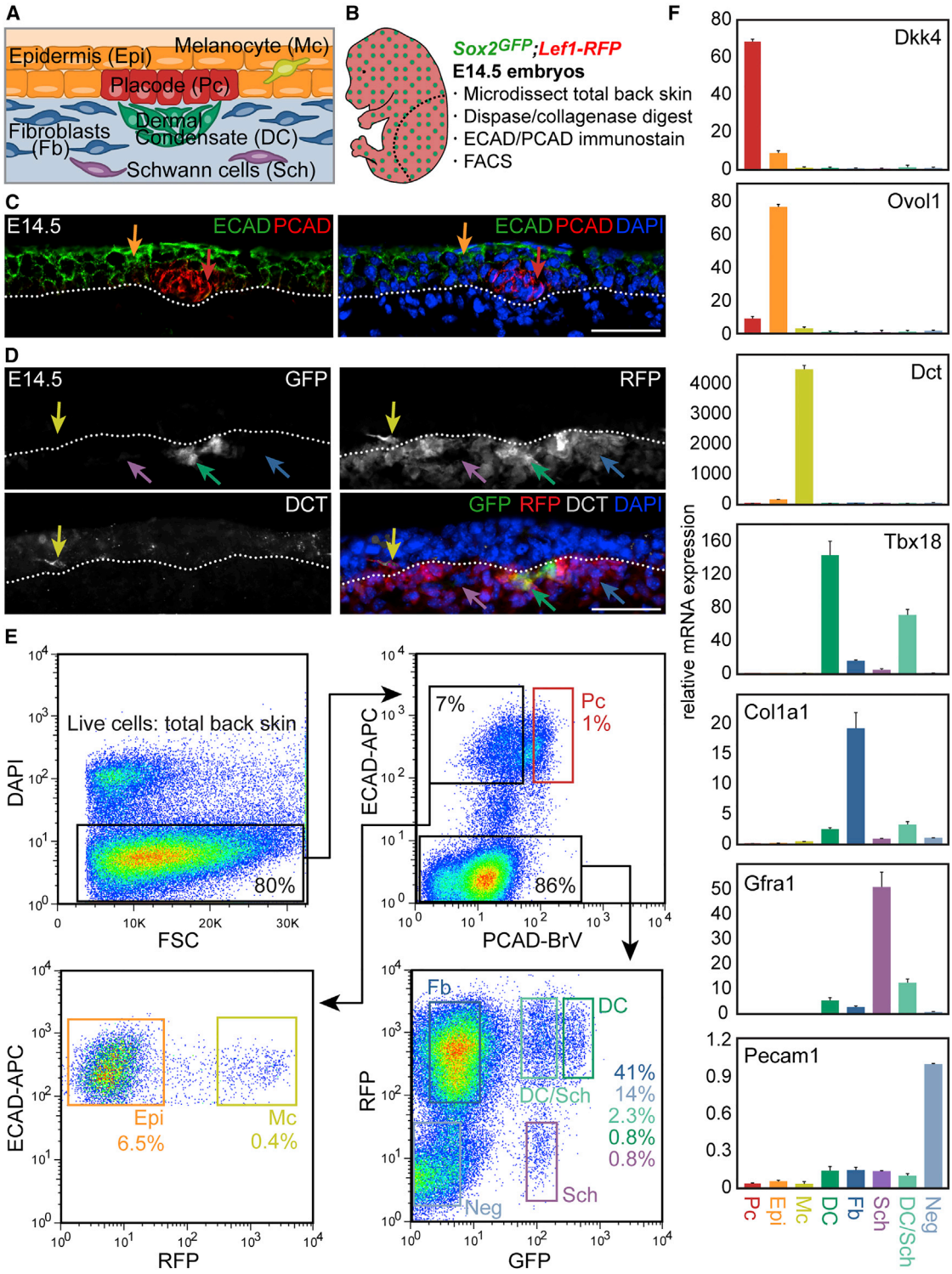

Figure 1. Multicolor Cell Sorting of Embryonic HF Progenitors, Niche, and Key Skin Cell Populations

(A) Schematic of E14.5 skin with early-stage HF.

(B) Outline of cell-sorting strategy from E14.5 *Sox2*^{GFP}/*Lef1-RFP* double-transgenic skin. Diagram illustrates the back skin area microdissected for analysis.

(C) Immunofluorescence staining for ECAD marks all epithelial cells (Epi, orange arrow), and PCAD is highest in Pc cells (red arrow). Dotted line demarcates basement membrane. DAPI highlights all nuclei.

(D) *Sox2*^{GFP}/*Lef1-RFP* E14.5 back skin includes GFP^{+}/RFP^{+} DC (green arrow), GFP^{-} RFP^{+} Fb (blue arrow), and GFP^{low}RFP^{-} Sch (purple arrow) cells; immunofluorescence for DCT confirms that RFP^{+} cells in the epidermis are Mc (yellow arrow).

(legend continued on next page)

important for directing hair growth and patterning through distinct mechanisms.

To systematically investigate the cellular complexity of developing embryonic skin and gain comprehensive insights into the molecular identity of HF progenitors and niche cells compared to non-hair-inducing keratinocytes and fibroblasts, we conducted refined cell isolations and genome-wide transcriptome analyses by RNA sequencing. Using double-transgenic reporter mice and specific antibodies, we isolated six distinct cell types from embryonic E14.5 mouse back skin, including Pc progenitors and DC niche cells, as well as lineage-related epidermal keratinocytes (Epi) and Fb, melanocytes (Mc), and Schwann cells (Sch), along with a mixed population comprising all remaining skin cells. Therefore, any gene expressed in E14.5 skin can be attributed to a specific cell type and/or compartment using our inclusive gene expression atlas. We composed a molecular snapshot of an entire tissue with unprecedented cellular resolution and mapped feasible modes of communication between specific cell types within the skin as HF formation begins. We further defined specialized signature expression profiles for each isolated cell type, composed of genes with the potential to control cell fates and, in turn, specific functionalities. With this work, we share our data in an integrative, searchable web database that enables the discovery and localization of genes of interest for further investigation. Our hope is that this publically available resource prompts the inception of additional studies so that the underlying molecular mechanisms of HF formation and skin development, including progenitor/niche fate acquisition and maintenance, will be further elucidated.

RESULTS

Isolation of HF Pc Progenitors, DC Niche Cells, and Other Distinct Cell Types from Embryonic Skin

The first cellular constituents of new HFs are epithelial Pc cells that give rise to activated matrix progenitors and future bulge SCs of downgrowing HFs and DC cells that form the future DP and dermal sheath niche. To gain comprehensive insights into the molecular makeup of these specialized cells, we devised an innovative multicolor labeling and cell-sorting strategy to purify Pc progenitors and DC niche cells during the first wave of HF morphogenesis at embryonic day (E)14.5 (Figure 1A). By simultaneously co-isolating Epi, Fb, Mc, and Sch and a population that contains all remaining skin cells (Neg), including an enrichment of endothelial and smooth muscle cells, we sought to define the unique molecular features of the progenitors and niche, along with other distinct cell types within the entire embryonic skin (Figure 1A). To this end, we used a combinatorial approach of double-transgenic reporter mice with immunofluorescence staining of single-cell preparations from E14.5 total back skin, followed by fluorescence-activated cell sorting (FACS) (Figure 1B). First, we crossed *Sox2*^{GFP} mice that express GFP under the endogenous *Sox2* promoter (Ellis et al., 2004) with *Lef1-RFP* mice that were engineered to express red fluorescent protein (RFP) under a human Lef1 promoter fragment (Rendl et al., 2005). *Sox2* is expressed in the mature DP and in embryonic DC niche precursors (Biernaskie et al., 2009; Driskell et al., 2009; Rendl et al., 2005; Tsai et al., 2010), and *Lef1-RFP* was previously used to isolate DP cells (Greco et al., 2009; Rendl et al., 2005). To simultaneously label all epithelial cells, including Pc, we performed double-immunofluorescence staining for the cell-surface markers E-cadherin (ECAD) and P-cadherin (PCAD) (Figure 1C). PCAD immunofluorescence was previously used at E17.5 to obtain a mixed population of Pc, downgrowing hair germ and hair peg cells from different HF formation waves (Rhee et al., 2006). At the earliest stage of first-wave HF formation at E14.5, we found the highest PCAD expression specifically in Pc, while ECAD was expressed by all epidermal cells. For the dermal compartment, GFP was strongly expressed in the DC cells of E14.5 *Sox2*^{GFP}*;Lef1-RFP* embryos (Figure 1D), as previously described (Clavel et al., 2012; Tsai et al., 2014). RFP was present in the DC and also broadly labeled Fb throughout the dermis (Figure 1D). In addition, RFP was expressed within the epidermal compartment in Mc, identified by co-expression of the marker DCT (Figure 1D). RFP$^+$ Mc also expressed the cell-surface marker ECAD, allowing their distinction from RFP$^+$ECAD$^+$ DC and Fb cells (Figure S1C). Additional combinations of immunofluorescence staining on GFP/RFP skin for ECAD, PCAD, or DCT, together with the basement membrane marker *Integrin-β4* (ITGB4), confirmed correct labeling and identification of each cell type (Figure S1A–S1C). In summary, our identified configuration of reporter and marker expression provided the necessary framework to proceed with cell isolations.

To purify all cell types by FACS, we first microdissected total back skin from E14.5 *Sox2*^{GFP}*;Lef1-RFP* embryos and released all skin cells by combined dispase/collagenase digestion. Trypsin digestion was not required to obtain single cells, and its omission allowed preservation of cell-surface antigen detection (data not shown). Then, we performed ECAD (allophycocyanin, APC)/PCAD (Brilliant Violet, BrV) double-immunofluorescence staining on a single skin preparation, followed by DAPI staining to label dead cells. Finally, all DAPI$^-$ live cells were subjected to the following nested FACS scheme to purify a total of eight separate cell populations encompassing the entire E14.5 embryonic skin (Figure 1E): ECAD shifted all epidermal cells with a further distinction by PCAD to isolate (1) ECAD$^+$PCAD$^+$ Pc (1% of live cells). The ECAD$^+$PCAD$^-$ gate included a mix of Epi and Mc cells, which were differentiated on the basis of RFP expression to purify (2) ECAD$^+$RFP$^-$ Epi (6.5%) and (3) ECAD$^+$RFP$^+$ Mc (0.4%) cells. ECAD$^-$ cells were >80% of total back skin and included a mix of dermal subpopulations distinguishable by varying levels of GFP and RFP. Consistent with what we observed in sections, ~0.9% of cells in the dermis highly expressed GFP and RFP, representing the (4) GFP^{High}RFP$^+$ DC compartment. (5) GFP$^-$RFP$^+$ Fb that exclusively expressed RFP made up ~46% of the cells in the dermis. What had not been easily apparent from sections alone was the existence of cells expressing low levels of GFP that were either

(E) FACS plots and gates for cell sorting. Starting from live cells, eight distinct gates mark HF progenitors, niche cells, four other specific cell types, and two mixed cell populations inclusive of the entire embryonic back skin.

(F) qRT-PCR for known marker genes demonstrates high enrichment for each purely isolated cell type. Data are means ± SD from two measurements.

Scale bars, 50 μm in (C) and (D). See also Figure S1.

(6) $GFP^{Low}RFP^{+}$ (2.3%) or (7) $GFP^{Low}RFP^{-}$ (0.8%). In addition, with flow cytometry, it became clear that 14% of live cells represented a (8) $GFP^{-}RFP^{-}$ (Neg) population. To account for all cells of the entire E14.5 skin and obtain a complete molecular snapshot at the genome-wide level, we collected these cells and defined their identity through marker gene explorations, as described later.

Next, we performed qRT-PCR to test the expression of known marker genes in the correct corresponding sample (Figure 1F; Figures S1D and S1E). As expected, Pc genes *Dkk4*, *Pcad*, *Shh*, *Wnt10b*, and *Edar* were highly expressed by isolated Pc cells compared to all other samples, while the expression of Epi markers *Ovol1*, *Evpl*, and *Krt1* was highly enriched in Epi cells. Mc cells uniquely expressed *Dct*, *Mitf*, and *Mc1r*. From the dermal compartment, the DC expressed high levels of *Tbx18*, *Sox2*, *Bmp4*, *Trps1*, and *Nrp2*, while Fb cells were strongly enriched for known fibroblast markers *Col1a1*, *Lox*, and *Lrig1*. Expression of neural crest and Sch cell genes, including *Gfra1*, *Fabp7*, *Mpz*, and *Gap43*, by $GFP^{Low}RFP^{-}$ cells indicated that these were Sch cells in varying stages of maturation. qRT-PCR analysis revealed that $GFP^{Low}RFP^{+}$ cells expressed both DC and Sch genes but consistently to a lesser extent than each cleanly isolated cell type, indicating that this sample was a mix of both (DC/Sch). Finally, $GFP^{-}RFP^{-}$ Neg cells included both endothelial and smooth muscle cells, as evidenced by the exclusive expression of known marker genes *Pecam1* (*CD31*), *Flt4*, *Flk1*, and *Nos3*, and likely encompassed other stray dermal cells that we did not specifically investigate further. Taken together, our qRT-PCR marker analyses verified our sorting strategy and confirmed that we were accurately able to isolate embryonic HF progenitor and niche cells, along with four other specific cell types and two mixed-cell populations inclusive of the entire embryonic skin.

Genome-wide Transcriptome Analysis of Independently Isolated Skin Cell Types

In order to comprehensively examine the unique gene expression profiles of the isolated HF progenitors, niche cells, and other cell types at the genome-wide level, we turned to RNA sequencing (Figure 2A). Using the sorting strategy outlined earlier, we isolated all eight cell populations in two separate FACS sorts to obtain biological replicates. Using only 6 ng of total RNA, we first generated amplified cDNA (NuGEN Ovation RNA-Seq System), which faithfully maintained relative gene expression patterns, as determined by additional qRT-PCR comparisons to conventional cDNA (Figure S2A). We then produced cDNA libraries with unique barcoded adapters for each of the 16 samples (NuGEN Ovation Ultralow Library System) that were subsequently analyzed by next-generation multiplexed sequencing (Illumina HiSeq 2000). This approach resulted in a high-quality output, with a mean quality score (Q score) >30 and >90% perfect index reads for all samples (Figure S2B). On average, 55 million total reads and 48 million aligned reads were produced per sample (Figure S2C).

Next, we proceeded by mapping, aligning, and quantifying these reads to compute differentially expressed genes between all cell populations. By ANOVA, we identified a total of >7,500 genes that were significantly differentially expressed (false discovery rate [FDR] < 0.05) in at least one of the eight cell populations. To gain a first glimpse into the global similarities and differences of gene expression patterns between all embryonic HF progenitor, niche, and other skin cell types, we investigated their relatedness by calculating coefficients of determination (r^2). As expected, all replicates displayed the highest correlation among all comparisons ($r^2 > 0.97$) (Figure 2B). While Epi and Pc cells were closely related, the comparison of either sample to any other resulted in plot-wide low r^2 values. These data reflected the highly unique gene expression patterns that are shared by Epi and Pc cells but distinct from all others. Disregarding the mixed samples, DC cells and Fb were the next closely correlated cell types, with the comparison between Sch and Mc almost as tight. At the other end of the spectrum, DC and Mc samples were most dissimilar.

Next, we performed hierarchical clustering of the differentially expressed genes, allowing further grouping of genes and populations according to their expression patterns (Figure 2C). This analysis also established that all replicates clustered together (Figure 2D) and grouped epithelial Epi and Pc cells apart from dermal and neural-crest cell types. Closely related Fb and DC cells clustered on one side with the DC/Sch population, whereas neural-crest-derived Mc and Sch cells were clustered separately, and Neg samples localized to their own branch of the dendrogram. Principal-component analysis provided an additional way to calculate and visualize the relationship between the eight samples (Figure 2E). Again, and as expected, replicates grouped together, with Pc and Epi localized closely in their own space. Neural-crest-derived Sch and Mc samples associated near the bottom of the plot, while Fb cells accompanied DC in a separate corner. The DC/Sch samples appropriately appeared between the two purely isolated cell types, while the Neg samples were located separately.

Finally, gene ontology (GO) analysis of the differentially expressed genes across all cell types revealed significant enrichment for genes related to signaling and migration (Figure 2F), highlighting the central roles of intercellular crosstalk and dynamic cell rearrangement in promoting skin and hair development.

Genome-wide Gene Expression Analysis Corroborates Previously Established Gene Markers

Several prior studies have examined the expression and functional role of specific genes in Pc and DC cells during HF morphogenesis at E14.5 (Ahn, 2015; Biggs and Mikkola, 2014; Sennett and Rendl, 2012). Global gene expression in embryonic Epi and Mc cells has been explored by microarray analysis, and expression of selected genes was examined in more detail (Bazzi et al., 2007a; Colombo et al., 2012). Further, several genes mark Sch cells at precise developmental stages (Jessen and Mirsky, 2005; Woodhoo and Sommer, 2008) and define heterogeneity in embryonic Fb (Driskell et al., 2013). To further validate the findings from our RNA-seq analysis we examined the fold expression changes of known marker genes from the established literature by comparing their FPKMs (fragments per kilobase of exon per million fragments mapped) in a target sample with those of its most closely related cell type (Figure 3). All examined marker genes were highly enriched in the correct cell type, supporting the accuracy of our isolation strategy and subsequent expression analysis methods. Additionally, we verified the marker

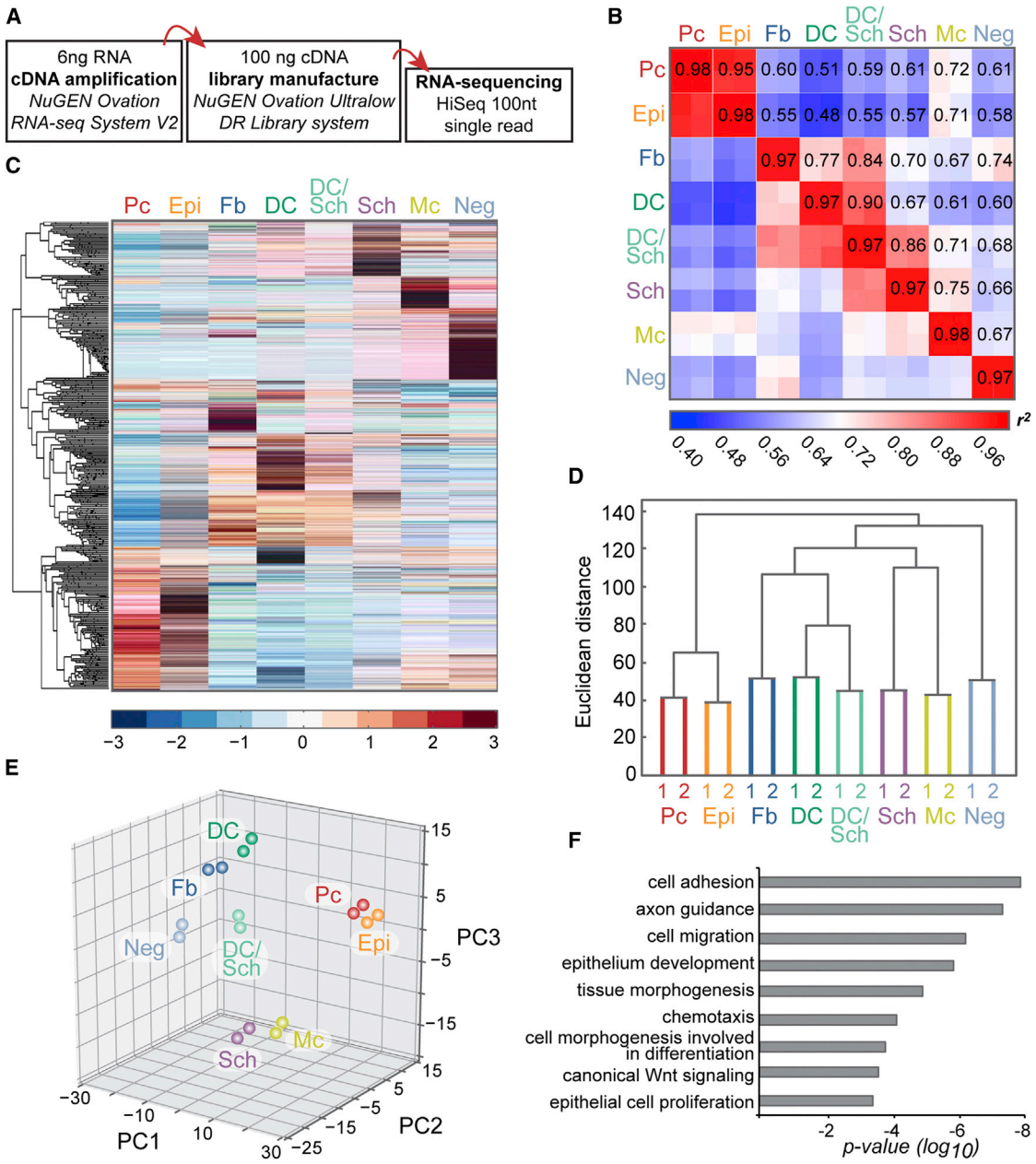

Figure 2. Cell Population-Level Analyses of RNA-Sequencing Data from Embryonic Skin Cell Types

(A) Workflow of sample preparation for RNA sequencing.

(B) Heatmap of coefficient of determination (r^2) for gene expression profiles of all isolated cell populations.

(C) Hierarchical clustering of differentially expressed genes. Heatmap illustrates distinct clusters of enriched gene expression in all isolated embryonic skin cell types.

(D) Hierarchical clustering analysis of embryonic skin cell populations. Biological replicates cluster together. Epithelial, mesenchymal, and neural-crest-derived cells group separately. y axis, Euclidean distance.

(E) Principal-component analysis with PC1 (43.74% variance captured), PC2 (16.97% variance captured), and PC3 (15.81% variance captured).

(F) GO analysis for differentially expressed genes. Shown are significantly overrepresented functional categories in embryonic skin.

gene expression pattern for select genes by qRT-PCR. Interestingly, the fold enrichment observed by qRT-PCR was frequently much greater than by FPKM comparisons, indicating that even minor but significant differences in gene expression found by sequencing could identify uniquely localized signature genes.

Defining Distinct Molecular Signatures of Embryonic HF Progenitors and Their Niche alongside Other Components of Developing Skin

Because unique expression of genes in a given cell type predicts functional relevance, we next defined cell-type-specific

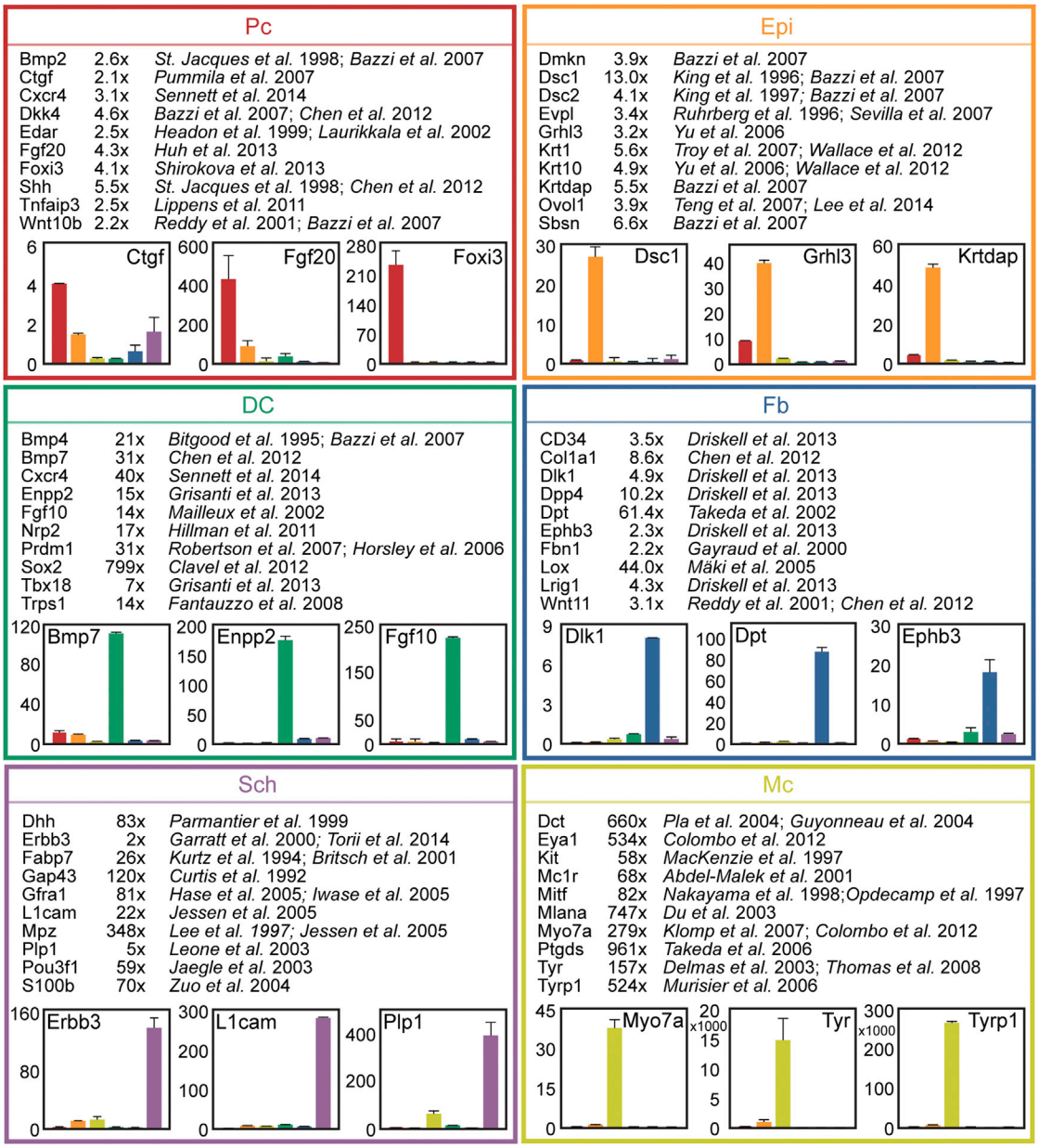

Figure 3. Comprehensive Representation of Known Cell-Type-Specific Markers

Established markers are appropriately enriched in the RNA-sequencing dataset. Ten representative marker genes and the relevant references are shown for each cell type. Numbers are fold change in FPKM difference between Pc versus Epi, DC versus Fb, and Sch versus Mc. qRT-PCR verification on independently sorted cells confirmed cell-type-specific gene expression. Data are means ± SD from two measurements.

molecular signatures for each of the six cleanly isolated skin cell populations (Pc, Epi, Mc, DC, Fb, and Sch). For this, we compared the FPKMs of all genes that were significantly differentially expressed across all samples or between any sample pairs, and genes expressed with FPKM > 1 and at 2-fold greater levels in one sample compared to all others were labeled signature genes (Figure 4A, non-overlapping sections). For the Pc versus Epi and the DC or Sch versus mixed DC/Sch comparisons, we applied a 1.5-fold cutoff, given the highly overlapping nature of these gene expression profiles. In total, we identified 1,728 signature genes for all six cell types, ranging from 102 genes in Pc cells to 395 genes in DC cells (Figure 4A; Table S1). Additionally, we classified highly enriched genes specific to cells categorized by epithelial, mesenchymal, or neural crest origin, compared to all other six cell populations (Figure 4A, intersections). 336 epithelial genes were shared by Pc and Epi cells, while 146 distinct dermal genes were expressed by DC and Fb cells. Finally, 67 genes overlapped between neural-crest-derived Mc and Sch cells (Table S2).

To gain global mechanistic insights into how each cell type might function during hair and skin formation, we next computed the enriched GO terms of all gene signatures (Figure 4B; Table

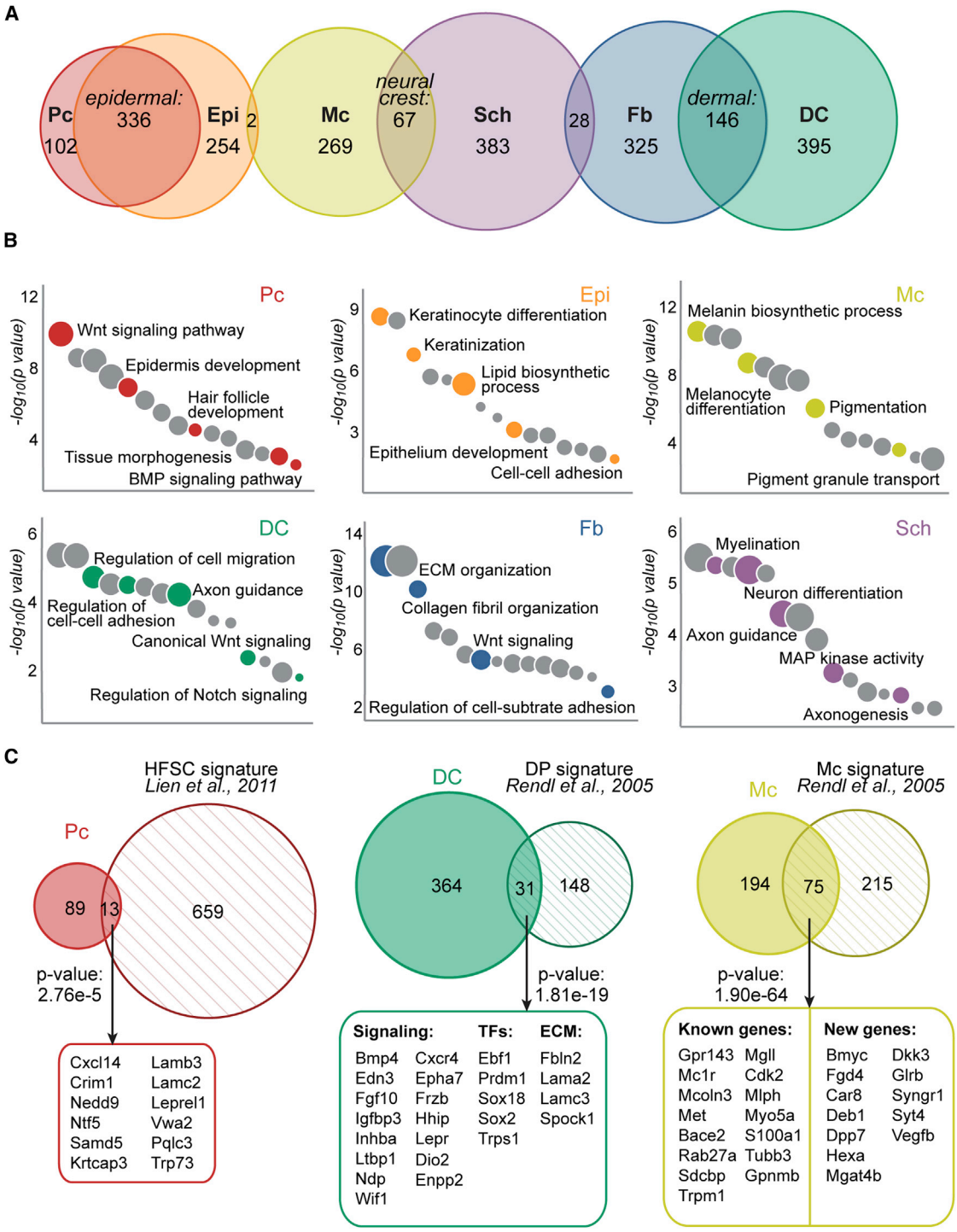

Figure 4. Molecular Signatures of Embryonic HF Progenitors, Niche Cells, and Other Key Embryonic Skin Cell Types

(A) Venn diagrams of cell-type-specific gene expression signatures. The overlaps represent genes enriched in epithelial, mesenchymal, and neural-crest cell types compared to all other populations. Note reduced overlap in unrelated cell lineages. Specific gene lists are provided in Tables S1 and S2.

(B) Gene ontology analysis of cell-type-specific gene signatures. Circle size corresponds to the number of genes related to each functional category within each signature list. Notable terms are highlighted; all terms are listed in Table S3.

(C) Embryonic gene signatures in comparison to previously published signatures of related cell types from adult HFs, with select common factors listed. All common factors are listed in Table S4. Statistically significant overlap was calculated with Fisher's exact test.

See also Tables S1, S2, S3, and S4.

S3) using Enrichr (Chen et al., 2013). Genes relevant to Wnt receptor signaling were highly associated with both Pc and DC signatures, consistent with the known central role of this pathway in promoting HF development (Andl et al., 2002; Chen et al., 2012; Reddy et al., 2001; Tsai et al., 2014; Zhang et al., 2009). Genes that promote epithelial cell differentiation were well represented in the Epi signature, in addition to genes related to keratinization and lipid biosynthetic processing. In the Fb signature, genes related to adhesion and extracellular matrix (ECM) organization prevailed. GO analysis of highly specialized Mc and Sch cells revealed equally distinct gene categories such as pigmentation or axonogenesis/myelination, respectively. Genes related to migration, adhesion, and signaling were highly represented within the DC signature, and, notably, several top hits were related to neural development and axon guidance. This observation was previously made for mature DP cells of postnatal follicles as well (Rendl et al., 2005).

Finally, we explored how embryonic progenitor and niche gene signatures were related to their mature postnatal counterparts. Several prior studies established gene signatures of cells within the SC niche during HF growth and/or the regenerative hair cycle. Lien et al. (2011) defined gene signatures for HF SCs at multiple points during the hair cycle using microarray technology and established an overarching adult SC signature consisting of 672 genes. From 102 embryonic Pc signature genes, a total of 13 genes (13%, $p < 0.001$) overlapped with the adult HF SC signature (Figure 4C; Table S4). These common genes largely have been unexplored so far in either Pc or adult HF SC function and are discussed in more detail later. A separate study examined genes unique to DP niche cells, the progeny of embryonic DC cells, in addition to establishing signatures of Mc and HF progenitor subtypes in growing HFs of postnatal day (P)5 mouse back skin (Rendl et al., 2005). Out of 395 signature DC genes, 31 (8%, $p < 0.001$) overlapped with the postnatal DP signature (Figure 4C). Intriguingly, many common genes were related to cell-cell signaling, and while several have been explored regarding condensate function during HF formation (*Sox2*, *Enpp2*, and *Cxcr4*), many have been newly identified and are discussed in the following text. Interestingly, many genes were shared between embryonic and postnatal Mc, with 75 of 269 (28%, $p < 0.001$) embryonic Mc signature genes also specifically expressed by postnatal Mc. The overlap included well-established Mc markers but also identified new common genes. In summary, with genome-wide sequencing, we defined comprehensive molecular signatures of embryonic HF progenitors, the niche, and other key cell types within the embryonic skin.

Many New Signature Genes Typify Unique Molecular Characteristics of Pc and DC Cells in Embryonic HFs

In addition to successfully detecting established Pc and DC genes (Figure 3), our analyses revealed many enriched genes that were not previously examined in embryonic mouse skin (Figure 5A; Table S1). In Pc, many such signature genes were related to cell communication and, specifically, modulation of canonical signaling pathways. Pc ligand *Pthlh* binds to receptor *Pth1r*, highly expressed in DC and Fb cells, is known to be important for the formation of mammary glands and teeth, and likely plays a role in mediating epithelial-mesenchymal interactions during skin/hair development as well (Hiremath et al., 2012; Philbrick et al., 1998). *Pthlh* specifically modulates mesenchymal bone morphogenetic protein (BMP) signaling, a pathway that needs precise regulation for HF formation to occur (Botchkarev et al., 1999; Jamora et al., 2003). *Crim1*, a factor with potential to be expressed extracellularly or secreted to affect VEGF (vascular endothelial growth factor), BMP, PDGF (platelet-derived growth factor), and TGFβ (transforming growth factor β) signaling, was found within the Pc signature and also overlapped with the published HF SC signature. *Dkk4* is a Wnt signaling inhibitor known to be highly expressed in the Pc (Bazzi et al., 2007b), but, interestingly, co-receptor *Kremen2* was found highest expressed in the Pc. *Scube3* was also found in the Pc signature and is a secreted factor that activates TGFβ signaling by interacting with *Tgfbr2*, highly expressed by DC, Sch, and Fb cells. Finally, because Wnt signaling within the epithelium is necessary to drive HF formation (Chen et al., 2012), it was interesting to note the presence of lone frizzled receptor *Fzd10* in the Pc gene signature.

Aside from canonical signaling factors, genes representing other signaling modalities were found enriched in the Pc signature. Gap junction genes *Gjb2* (*Cx26*) and *Gjb6* (*Cx30*) were both enriched and are known to form heterodimeric channels to facilitate communication between linked cells, representing one way that Pc progenitors might coordinate their activity as a unit. Another signature gene, *Syt7*, a calcium-sensing member of the synaptogramin family, facilitates signaling by promoting vesicle fusion and exocytosis of secreted factors. Prostaglandin signaling could play a role in coordinating skin formation, as synthase *Ptges* was highly expressed in the Pc, and Ptge receptors were present in both Epi and Fb cells. Intracellular components important for transducing signals were uniquely expressed in the Pc as well, including *Nedd9*, which was found highly expressed in both Pc and adult HF SC signatures. Another example, *Art4* (*CD297*), regulates NAD metabolism to promote signaling through multiple cascades. Finally, *Ifitm3* is a receptor known to be involved in interferon signaling and was also identified as a highly expressed gene within the Pc signature in E14.5 skin.

A number of transcription factors were found differentially expressed in the Pc compared to interfollicular Epi. *Ascl4* is a basic-helix-loop-helix (bHLH) transcription factor and, although not well studied, has been implicated in skin development because of its restricted, high expression in fetal skin (Jonsson et al., 2004). Another uniquely expressed transcription factor was *Sox21*, previously characterized in cells of the growing hair cuticle (Kiso et al., 2009). Expression of *Sox21* at E14.5 was not described in this previous study, but its ablation resulted in a severe, progressive alopecia, despite what appeared to be normal hair formation through the first week of life.

Multiple signature genes in the DC were similarly involved in cell-cell signaling, which could be particularly relevant in coordinating events during the earliest stages of HF formation. Canonical SHH and Wnt signaling pathway inhibitors *Hhip* and *Wif1*, respectively, were noticeably enriched in the DC signature. Overlap with the previously published postnatal DP signature suggests an essential role in condensate function during hair development. Curiously, indicators/potentiators of active SHH and Wnt signaling, including *Ptch1/2*, *Rspo3*, and *Wisp1*,

A

Pc

Signaling				Transcription	
Art4	1.9x	Nedd9	1.7x	Ascl4	5.0x
Bmpr1b	1.8x	Ntf5	3.0x	Foxb1	2.5x
Capsl	1.6x	Pm20d1	1.6x	Hoxc13	1.6x
Crim1	1.6x	Pqlc3	1.7x	Irx4	1.6x
Ctf1	1.5x	Ptges	1.6x	Sox21	2.0x
Cxcl14	1.9x	Pthlh	4.3x	Trp73	1.7x
Fzd10	1.7x	Rasgef1b	2.2x	Zfp473	2.2x
Gjb2	2.1x	Samd5	1.6x		
Gjb6	1.7x	Scube3	1.6x	**Structure**	
Ifitm3	1.5x	Slc25a48	2.1x	Chst11	2.0x
Kremen2	1.6x	Spink5	2.3x	Cldn7	1.6x
Leprel1	1.6x	Susd4	1.8x	Fry	1.6x
Lgi2	2.3x	Syt7	1.6x	Krt7	2.3x
Mapk4	2.3x	Vwa2	1.6x	Krtcap3	1.6x

Epi

Signaling		Enzymes	
Ace2	5.5x	Acsl1	4.2x
Ano7	5.9x	Aldh1a7	8.8x
Bspry	4.1x	Faah	10.3x
Dkkl1	15.5x	Gsta2	7.2x
Ly6g6e	6.7x	Mgst1	4.7x
Paqr5	4.4x	Mgst2	8.7x
Pla2g4f	10.6x	Sdr16c5	7.4x
Prrg4	3.5x	Them5	5.5x
Ptger3	4.1x	Tmprss4	10.1x
Rbp2	76.8x	**ECM/ adhesion**	
S100a14	4.4x	Ceacam19	8.0x
Transcription		Dlg2	3.9x
Dlx5	3.8x	Gjb5	7.6x
Spib	2.7x	Muc15	6.5x

Mc

Signaling		Secretion	
Cck	xx	Adcy9	20.3x
Dkk3	4.0x	Bnc2	49.3x
Fabp3	15.3x	Ctsd	3.3x
Gpm6a	11.3x	Cubn	65.0x
Plxnc1	6.5x	Nostrin	31.3x
Trim63	366.0x	Plcb4	4.2x
Vegfb	4.6x	Rapgef4	42.5x
Transcription		Scamp1	7.6x
Aff3	9.5x	Sirpa	12.4x
Alx1	113.2x	Tpp1	2.7x
Bhlhe41	342.5x	**ECM/ adhesion**	
Elf2	2.3x	Cd274	19.2x
Hsf4	55.5x	Cldn10	25.1x
Scml4	77.1x	Fmn1	43.4x

DC

Signaling		Transcription		ECM/ adhesion	
Dcc	7.6x	Alx4	13.8x	Adam22	2.5x
Ephb1	25.3x	Bcl6	15.5x	Adamts18	299.8x
Gal	735.1x	Ebf4	4.1x	Adamts4	10.1x
Hhip	10.7x	Foxd1	224.7x	C1qtnf1	7.8x
Igf1	7.4x	Glis2	5.0x	CD97	2.9x
Lynx1	51.8x	Klf4	6.5x	Col19a1	60.9x
Ndnf	26.8x	Mxi1	6.1x	Gpc2	5.1x
Robo1	2.9x	Sox18	304.1x	Ibsp	314.1x
Rspo3	7.6x	Sox9	14.8x	Lgals1	2.2x
Sema6a	4.5x	**Neuronal**		Pcsk5	5.3x
Spry1	4.3x	Cdh4	5.9x	Pdlim3	165.9x
Sstr2	116.3x	Dclk1	13.2x	Smoc1	37.9x
Unc5b	4.4x	Grin2a	863.3x	Spock1	16.6x
Wif1	2.6x	Ntf3	11.4x	Spon2	6.2x

Fb

Signaling		Transcription	
Fzd1	6.9x	Emx2	9.9x
Grem1	35.5x	Gata6	41.2x
Grem2	36.9x	Irx1	20.0x
Inhbb	18.4x	Osr2	46.3x
Lpar1	12.3x	Pou3f3	66.1x
Mme	3.0x	Sim1	47.7x
Ntn1	14.0x	**ECM/ adhesion**	
Ptgfr	23.4x	Adam33	26.1x
Rspo1	11.1x	Col12a1	9.0x
Sema5b	10.9x	Col24a1	13.4x
Sfrp5	8.0x	Col8a1	12.2x
Slit2	2.7x	Efemp1	47.5x
Thbs1	7.7x	Pcolce	9.6x
Thbs2	42.8x	Ptn	40.0x

Sch

Signaling		Neuronal	
Dab1	12.7x	Fign	8.4x
Deptor	2.6x	Gabra2	670.9x
Dkk2	120.1x	Gas7	12.5x
Ecel1	743.0x	Luzp2	63.8x
Lect1	218.7x	Ntrk3	14.19x
Moxd1	161.3x	Plxnb3	265.6x
Reln	152.2x	Sema3g	11.2x
Sstr1	924.8x	Slitrk2	58.5x
Transcription		Vat1l	83.1x
Dlx1	427.8x	**ECM/ adhesion**	
Dlx2	xx	Cdh6	141.1x
Foxo1	2.3x	Cntn6	824.0x
Hoxb9	82.7x	Igsf11	2.1x
Nr2f1	35.7x	Lims2	23.7x

B

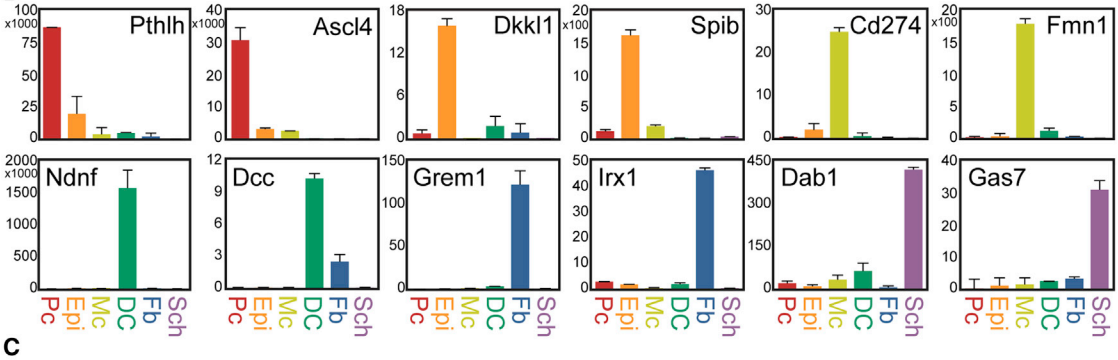

C

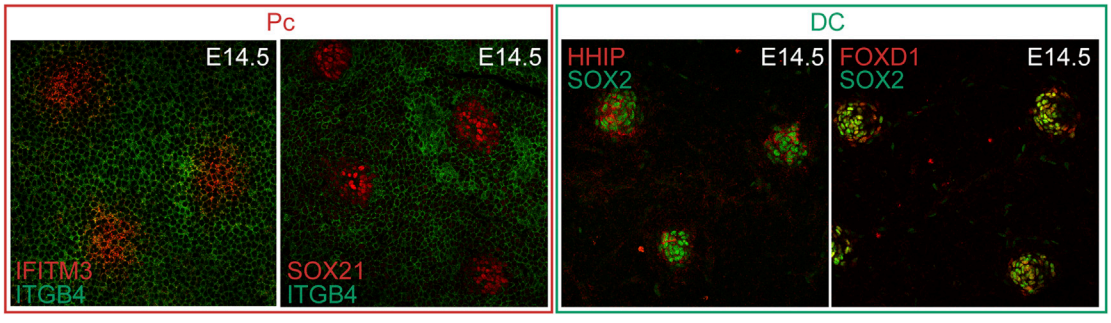

Figure 5. Cell-Type-Specific RNA Sequencing Reveals Many New Signature Genes

(A) Select enriched genes for each cell type are listed along with the fold change of gene expression as measured by FPKM. Fold change is measured as Pc versus Epi, DC versus Fb, and Sch versus Mc. Genes are organized according to functional categorization. FDR of $q < 0.05$ for all genes.

(B) qRT-PCR verification of select signature genes for each cell type. Data are mean ± SD from two measurements.

(C) Immunofluorescence staining verification of selected signature genes for the Pc and DC. Whole-mount view of E14.5 skin.

See also Figure S3.

were also uniquely expressed in the DC signature. Similarly, while fibroblast growth factor (FGF) signaling inhibitors *Spry1* and *Fgfrl1* were highly expressed in the DC signature, so was activating ligand *Fgf10* (Suzuki et al., 2000). Previous reports have highlighted the role of the DP in fine-tuning cell-cell signaling during hair growth (Clavel et al., 2012); it seems likely that the DC has a similar function during hair development.

More obscure signaling factors expressed exclusively in DC cells in embryonic skin included *Ndnf* (also known as *Epidermacan*), a relatively unexplored secreted factor; *Dclk1*, a kinase implicated in neural cell migration; *Grin2a*, an NMDA receptor subunit important for synaptic transmission; and *Syt6*, another member of the synaptogramin family instrumental in vesicular exocytosis and signaling execution. *Pcsk5* is also important for the mechanics of signaling as an enzyme that activates proproteins via site-specific cleavage, and its substrates include peptide hormones and adhesion molecules that could influence signaling through DC-cell contacts.

In addition to factors related to signaling, numerous transcription factors were unique to the DC gene signature. Interestingly, multiple Sox transcription factors were found enriched in the DC. The expression and function of *Sox2* is well established in the DP (Clavel et al., 2012; Driskell et al., 2009), but this analysis additionally highlighted the localized expression of both *Sox9* and *Sox18* in E14.5 DC. As these Sox genes belong to separate Sox family subgroups, they likely act non-redundantly to influence condensate cell activity and maturation. *Foxd1*, a forkhead box transcription factor with a known role in kidney development, was especially enriched in DC compared to Fb cells (Fetting et al., 2013). Kruppel-like zinc finger *Glis2*, extensively studied for its role in kidney development as well, was identified in the DC signature, while related protein *Glis1* was also highly expressed in these cells. Both factors can act as transcriptional activators or repressors to influence a multitude of other intracellular signaling cascades.

The few genes described here represent only a small fraction of the most interesting new signature genes of Pc and DC. qRT-PCR and immunofluorescence for select genes verified expression at the RNA and protein levels (Figures 5B, 5C, and S3). In total, we confirmed enrichment of over 200 genes within Pc, Epi, Mc, DC, Fb, and Sch signatures by qRT-PCR (total of 82 genes shown in Figures 1, 3, 5, S1, and S3). Our sampling approach to verify the sequencing data substantiated virtually all inspected signature genes, and the few factors highlighted in Figure 5 provide only a small glimpse of the hundreds of new signature genes defined for multiple cell types in embryonic skin by our inclusive and in-depth experiments (Table S1).

Distinct Expression Patterns of Genes Related to Canonical and Other Defined Signaling Pathways, Including Axon Guidance Signaling, in Embryonic Skin

Many signature factors in multiple cell types of embryonic skin were related to canonical signaling pathways Wnt, SHH, TGFβ, and Notch, among others (Figures 4B and 5A) and have been studied in the context of Pc and DC crosstalk in great detail (Lee and Tumbar, 2012; Wang and Wu, 2014). To understand how canonical signaling factors might influence skin development on a broader scale, we constructed heatmaps to illuminate patterns of relevant gene expression for specific pathways between all six isolated cell types (Figure 6A; Figure S4A). Genes were mined from the Kyoto Encyclopedia of Genes and Genomes (KEGG) pathway database (Kanehisa and Goto, 2000; Kanehisa et al., 2014) and were included in the maps as long as they were expressed (FPKM > 1) by one of the six cell types included in the analysis.

This illustrative strategy made it easily apparent that, in the case of Wnt signaling, most ligands were expressed from the epithelial compartment, with especially high expression in the Pc. The exceptions were non-canonical *Wnt11* and *Wnt5a/5b*, expressed strongly by DC and Fb cells. Multiple Wnt signaling inhibitors were also expressed highly in the dermal compartment, including *Dkk1*, *Wif1*, and all *Sfrps*. In a separate map, *Fgf20* expression, known to be important for DC formation (Huh et al., 2013), was correspondingly strong from Pc, while *Fgfr1* expression was notably high in DC. Ligands, receptors, and downstream factors for BMP signaling were expressed in both epithelial and dermal compartments (Botchkarev and Sharov, 2004). BMP signaling inhibitors, including *Grem1*, *Grem2*, *Chrd*, and *Nog*, however, were strongly localized to Fb cells. Analysis of Notch signaling factors revealed strong and specific expression of *Notch* binding partner *Dll1* in DC cells. Although no single *Notch* was exclusively found in DC cells, downstream effector *Rbpj* and direct targets *Hes5* and *Hey1* were highly expressed. Finally, pathway analysis confirmed that *Shh* ligand was specifically produced by Pc cells, as has been well established (Chiang et al., 1999; St-Jacques et al., 1998), and that both *Ptch* and *Smo* receptors were strongly present in DC and Fb cells. Downstream effectors of SHH signaling, including *Gli1* and *Gli2*, were also expressed in DC cells. In summary, whole transcriptome analyses of embryonic HF progenitors, the niche, and other key skin cell populations enabled construction of detailed maps for multiple canonical signaling pathways and a comprehensive overview of each pathway's factors within embryonic skin.

Next, we used Enrichr (Chen et al., 2013) for KEGG pathway analyses to ascertain overrepresented signaling pathways in signature gene lists. Factors related to both SHH and Wnt signaling were prevalent in the Pc signature (Figure 6B; Table S5). General factors related to cell communication were found in both Pc and Epi signatures, while genes involved in melanogenesis were most significantly overrepresented in the Mc gene list. This analysis also revealed genes important for SHH, TGFβ, and P53 signaling within the DC signature. As described earlier, the roles of several canonical signaling pathways are well established in driving HF formation, although the importance of P53 signaling has yet to be addressed. In addition, KEGG analysis found that factors related to axon guidance were significantly overrepresented within the DC signature. Correspondingly, genes related to ECM interactions were highly and significantly present in the Fb signature, while ErbB signaling that is known to be important for Sch cell maturation was highlighted by KEGG analysis of the Sch signature.

The significant enrichment of genes related to axon guidance within the DC was particularly intriguing. On closer inspection, our analyses uncovered that both ligands and receptors important for signaling through Chemokine, Semaphorin, Neurotrophin, Neuropilin, Netrin, Ephrin, Slit-Robo, and SHH pathways were part of the DC signature (Figure 6C). Importantly, many

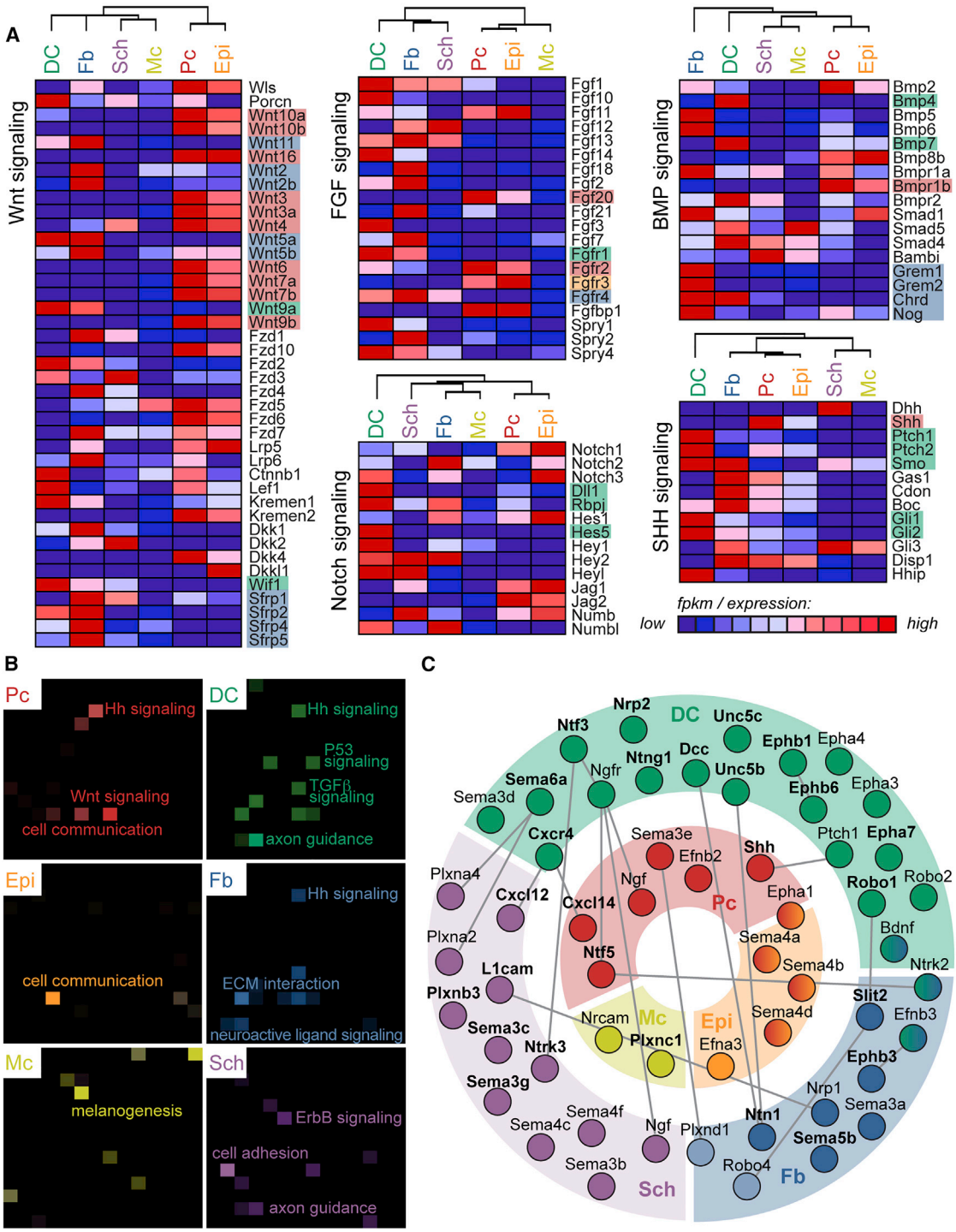

Figure 6. Genes from Defined Signaling Pathways Are Highly Expressed and Specifically Partitioned in Embryonic Skin

(A) Genes involved in Wnt, FGF, BMP, Notch, and SHH signaling were mined from the KEGG database and represented in the heatmap if expressed (FPKM > 1) in embryonic skin. Discussed genes are highlighted and color coded for cell type.

(B) KEGG pathway analysis (Enrichr) for each cell-type-specific molecular signature. Brighter tiles in the canvas indicate greater significance; notable terms are labeled. All terms and relevant genes are listed in Table S5.

(C) Signature (in bold) and other enriched genes related to axon guidance signaling are localized to specific cell types in embryonic skin. Connections indicate known interactions between two factors as mined from literature.

See also Figure S4 and Table S5.

corresponding ligands and/or receptors were highly expressed in neighboring Pc, Sch, or Fb cells. Overall, the prevalence of strongly expressed genes related to axon guidance signaling in multiple cell types within embryonic skin was apparent through GO analysis, KEGG pathway analysis, and inspection of signature gene lists, suggesting a functional role in promoting hair and skin development.

DISCUSSION

The notion that epithelial-mesenchymal crosstalk drives HF development, growth, and cycling has prompted investigations to establish gene signatures for adult SCs and the niche (Blanpain et al., 2004; Driskell et al., 2009; Greco et al., 2009; Lien et al., 2011; Morris et al., 2004; Rendl et al., 2005; Tumbar et al., 2004). However, only limited insights into the molecular makeup of their embryonic precursors have been generated by studies that isolated and profiled total epidermis (Bazzi et al., 2007a), a compound population of progenitors from different HF formation waves (Rhee et al., 2006), or condensate niche cells without collecting any other population for comparison (Tsai et al., 2014). Further, these prior studies were performed using microarrays that, while cutting-edge at the time, have been surpassed by unbiased deep-sequencing technology. To date, a comprehensive and refined analysis of embryonic precursors to both adult HF SCs and niche has been lacking, hampering the systematic discovery of molecular players coordinating HF morphogenesis. Here, we solve this problem with a high-resolution, in-depth exploration of gene expression in the earliest Pc progenitor and DC niche constituents of nascent HFs within the broader context of the entire embryonic skin. We co-isolated pure Pc and DC cells from the first HF development wave, in parallel with lineage-related Epi and Fb, neural-crest-derived Mc and Sch, and a population inclusive of all remaining cells within embryonic E14.5 skin (Neg). Rigorously comparing the genome-wide RNA-sequencing analysis of each isolated cell type or population captured a molecular snapshot of the whole tissue with unprecedented cellular resolution and precipitated signature gene discovery. Analyzing these signatures to assess GO and signaling pathway involvement revealed that factors related to axon guidance signaling were significantly represented in the DC signature and highly expressed in others, implying functionality in promoting the large-scale and dynamic cellular rearrangements that occur during HF formation.

Comparing the new embryonic signature gene lists to those previously published for adult HF SC and niche was particularly intriguing. As DC cells are precursors of postnatal DP niche cells (Grisanti et al., 2013a), shared genes likely confer niche cell identity or promote specialized hair-inducing functions. Meanwhile, the link between embryonic Pc progenitors and adult HF SCs is less clear cut. Fate-mapping *Shh*-expressing cells resulted in labeled progeny that contributed to the entire postnatal HF, including bulge SCs (Levy et al., 2005), suggesting that the Pc cells isolated in our experiments are, indeed, SC precursors. If so, the distinct signature lists of Pc and HF SCs reflect the disparate activities of an expanding progenitor pool compared to a mature, reserve SC compartment.

A notable strength of our sequencing strategy was the inclusion of all cells from a single preparation of total embryonic skin, categorized in terms of defined, isolated cell types accounting for the bulk of the skin (>85%), and one population encompassing all remaining cells. While gene expression analysis revealed that this fraction largely contained endothelial and smooth muscle cells, any dermal subpopulations that were as yet uncharacterized were enveloped in the mix. The advantage of collecting and sequencing this population means that any distinguishing gene for such a subpopulation should be exclusively confined to this fraction—and additionally ensuring that the signatures established for the purely isolated cell types are definitive markers for those cells within the total embryonic skin.

While the results of this study showcase an impressive number of new signature genes, our approach also allows a fresh and comprehensive look at previously published reports of specific genes expressed by Pc and DC in the context of the entire developing skin. Multiple studies, for example, have assessed the crucial role of the Wnt signaling pathway in promoting hair induction, formation, and growth. One such investigation systematically localized Wnt ligand expression in E14.5 skin, using tissue in situ hybridization, and our RNA-sequencing data on purely isolated cells are consistent with that report (Reddy et al., 2001). At the same time, our heatmap pathway analysis allows us to appreciate the relative localization of other components of the Wnt signaling pathway across all skin cell types, including receptors, inhibitors, and downstream effectors. This global approach enables a bird's-eye view not only of where important signaling factors are produced but also of where their message is received.

Pathway analyses additionally featured the enriched expression of factors related to axon guidance signaling in the DC signature gene list. Multiple receptors related to Slit-Robo signaling, including *Robo1*, *Unc5b*, and *Dcc*, were all found highly expressed by DC cells. Considering that Slit-Robo signaling confers repulsive information and that ligands *Ntn1* and *Slit2* were present in the Fb signature, this dialogue could be crucial for sorting specialized DC precursor cells from Fb. Neurotrophic factor *Ntf3* was part of the DC signature, with receptor *Ntrk3* enriched in Sch cells. A potential role for DC cells in guiding or maintaining Sch cell development in embryonic skin has not yet been explored. Other genes related to axon guidance signaling and highly expressed in DC cells were *Sema6a*, with *Plxn* ligands again enriched in Sch cells, and *Ephb1*, with ligand *Efnb*s expressed in multiple cell types. Interestingly, select axon guidance signals were also produced from the Pc, including *Ntf5* and *Cxcl14* that remarkably overlapped with the adult HF SC signature. *Ntf5* signals through receptors *Ngfr* and *Ntrk2*, enriched in DC and Fb cells, whereas *Cxcl14* binds DC signature gene *Cxcr4.*

Importantly, a main aim of this project is to share the gained information on a companion website to promote additional future discovery (Figure 7). This RNA-sequencing endeavor was conducted to provide a global tissue-level look at gene expression with cellular resolution encompassing several key cell types present in E14.5 skin, as HF formation is just starting. Seemingly, any gene identified here as specifically enriched in one cell type could be crucial to its unique functionality, but the task of investigating all signature genes is too great for any one lab to undertake alone. To promote the exchange of this information, we created a website with an easily searchable interface to act as a companion to this resource paper: the Hair Gene Expression

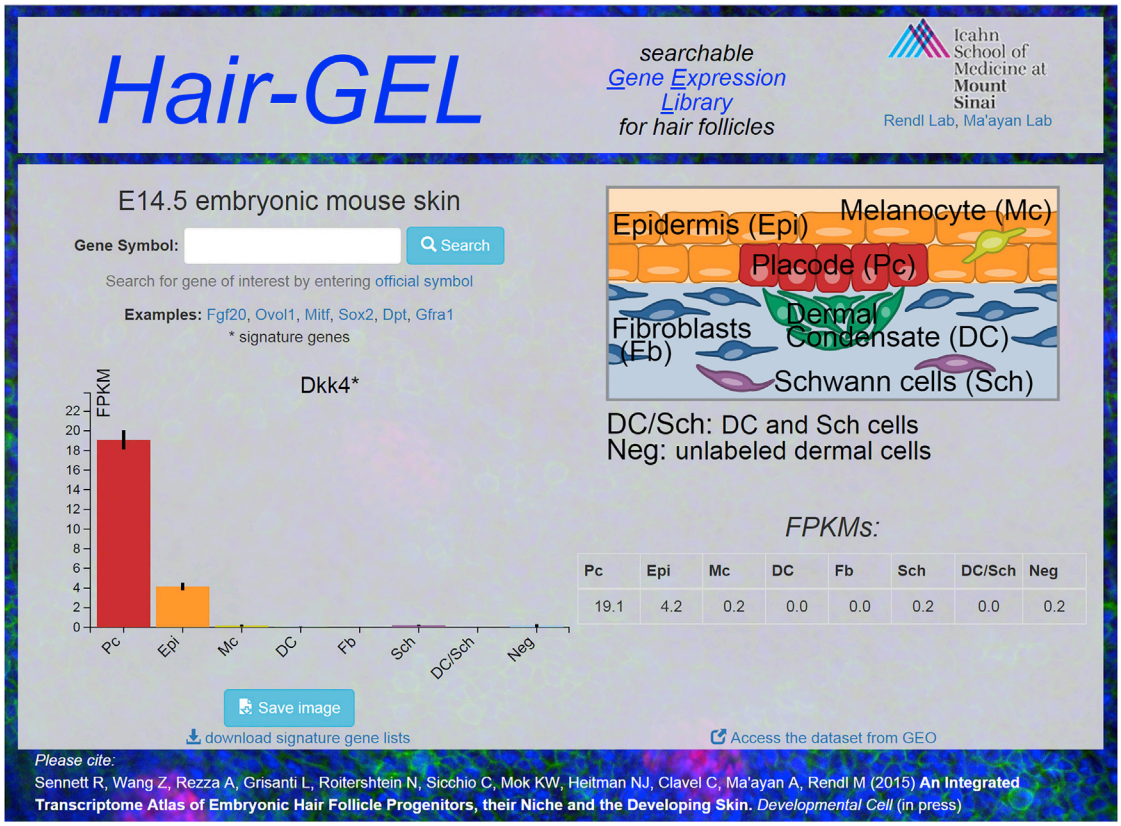

Figure 7. Hair-GEL: An Interactive, Searchable Online Gene Expression Library
Representative screenshot from companion website. The site hosts all raw data for download.

Library (http://hair-gel.net/). This website will be maintained and periodically updated as new information becomes available. Researchers can query any gene of interest to determine whether it is present and/or where its expression is most enriched within embryonic skin. Our ultimate hope is to inspire and enable additional studies that will further elucidate the complex molecular controls driving skin and hair follicle morphogenesis.

EXPERIMENTAL PROCEDURES

Mice

Sox2^{GFP} and *Lef1-RFP* mice were described previously (Ellis et al., 2004; Rendl et al., 2005), and the animals were housed in facilities operated by the Center for Comparative Medicine and Surgery (CCMS) at the Icahn School of Medicine at Mount Sinai (ISMMS). All animal experiments were conducted in accordance with the guidelines and approval of the Institutional Animal Care and Use Committee at the ICMMS.

Immunofluorescence Staining

Whole-mounted embryo skins or sections were fixed with 4% paraformaldehyde (PFA), washed with PBS, and then incubated with primary and secondary antibodies. Antibodies used included ECAD (rat, 1:100, Invitrogen), PCAD (goat, 1:100, R&D Systems), TRP2 (DCT) (goat, 1:100, Santa Cruz Biotechnology), ITGB4 (rat, 1:100, BD Pharmingen), EDAR (goat, 1:100, R&D Systems), KREMEN2 (goat, 1:500, R&D Systems), SOX21 (goat, 1:100, R&D Systems), HHIP (goat, 1:100, R&D Systems), or FOXD1 (goat, 1:100, Santa Cruz). After washes, samples were incubated with the Rhodamine Red-X-, AF488-, or DyLight 649-conjugated donkey anti-goat, -rat, or -rabbit secondary antibodies (Jackson ImmunoResearch). Nuclei were counterstained with DAPI. Slides were analyzed using a Leica SP5 DM confocal microscope driven by the Leica LASAF software.

Cell Isolation by FACS

To isolate cells from embryonic skin, *Sox2*^{GFP}*/Lef1-RFP* E14.5 embryos were processed as previously described (Tsai et al., 2014). Embryos were collected in ice-cold PBS, and back skins were harvested by microdissection. Skins were incubated in dispase (Invitrogen) with 0.2% collagenase (Sigma-Aldrich) and 20 U/μl of DNase (Roche) for 40 min at 37°C, filtered through 40-μm cell strainers, and then centrifuged at 350 × *g* for 5 min. Resuspended cell pellets were stained with primary antibodies against ECAD (rat, 1:250, Invitrogen) and PCAD (goat, 1:50, R&D Systems), followed by staining for secondary antibodies Donkey anti-rat APC (1:400, Jackson ImmunoResearch) and Streptavidin-Brilliant Violet 421 (1:200, Biolegend). DAPI was added for dead cell identification. Cell isolations were performed on a BD Influx cell sorter at the ISMMS flow core facility.

cDNA Generation, Library Manufacture, and RNA Sequencing

Total RNA obtained from FACS-sorted cells was purified with the Absolutely RNA Nanoprep Kit (Agilent), quantified with the NanoDrop spectrophotometer (Thermo Scientific) and measured for quality control using the Agilent Bioanalyzer. Samples with RIN (RNA integrity number) scores of 8.8 and higher were further processed. 6 ng starting material was reverse transcribed and amplified to 5–7 μg cDNA with the RNA Ovation RNA-Seq System V2 (NuGEN). From 100 ng amplified cDNA, sequencing libraries were generated with 16 unique barcoded adapters (8 samples × 2 replicates) using the Ovation Ultralow DR Library System (NuGEN). Library concentration and quality were quantified by Qbit (Invitrogen) and Bioanalyzer (Agilent) and subsequently sequenced on the Illumina HiSeq 2000 platform using a 100-nt single-read

setting. Details of RNA-sequencing analysis are provided in Supplemental Experimental Procedures.

Real-Time qRT-PCR

Total RNA obtained from FACS-sorted cells was purified with the Absolutely RNA Nanoprep Kit (Agilent), quantified with the NanoDrop spectrophotometer (Thermo Scientific), and reverse transcribed using oligo(dT) primers (Superscript III First-Strand Synthesis System, Invitrogen). Real-time qRT-PCR was performed with a LightCycler 480 (Roche) instrument with LightCycler DNA Master SYBR Green I reagents. Differences between samples and controls were calculated based on the $2^{-\Delta\Delta Ct}$ method and normalized to *Gapdh*. Measurements were recorded in duplicate. Primers used are listed in Supplemental Experimental Procedures.

ACCESSION NUMBERS

The accession number for the RNA-seq data reported in this paper is GEO: GSE70288.

SUPPLEMENTAL INFORMATION

Supplemental Information includes Supplemental Experimental Procedures, four figures, and five tables and can be found with this article online at http://dx.doi.org/10.1016/j.devcel.2015.06.023.

ACKNOWLEDGMENTS

We thank Valerie Horsley, Hoang Nguyen, and Robert Krauss for valuable comments on the manuscript. Many thanks also go to the personnel of the Flow Cytometry Core Facility and the Microscopy Shared Resource Facility at ISMMS. R.S. was supported by fellowship F30AR065847 from the National Institute of Arthritis and Musculoskeletal and Skin Diseases (NIAMS). A.M. was supported by NIH grants R01GM098316, R01DK088541, U54CA189201, and U54HL127624. M.R. was supported by grants from the NIAMS (R01AR059143, R01AR063151) and New York State Department of Health (NYSTEM-C029574) and by a fellowship from the Irma T. Hirschl Trust.

Received: April 7, 2015
Revised: June 4, 2015
Accepted: June 23, 2015
Published: August 6, 2015

REFERENCES

Ahn, Y. (2015). Signaling in tooth, hair, and mammary placodes. Curr. Top. Dev. Biol. *111*, 421–459.

Andl, T., Reddy, S.T., Gaddapara, T., and Millar, S.E. (2002). WNT signals are required for the initiation of hair follicle development. Dev. Cell *2*, 643–653.

Bazzi, H., Fantauzzo, K.A., Richardson, G.D., Jahoda, C.A.B., and Christiano, A.M. (2007a). Transcriptional profiling of developing mouse epidermis reveals novel patterns of coordinated gene expression. Dev. Dyn. *236*, 961–970.

Bazzi, H., Fantauzzo, K.A., Richardson, G.D., Jahoda, C.A.B., and Christiano, A.M. (2007b). The Wnt inhibitor, Dickkopf 4, is induced by canonical Wnt signaling during ectodermal appendage morphogenesis. Dev. Biol. *305*, 498–507.

Biernaskie, J., Paris, M., Morozova, O., Fagan, B.M., Marra, M., Pevny, L., and Miller, F.D. (2009). SKPs derive from hair follicle precursors and exhibit properties of adult dermal stem cells. Cell Stem Cell *5*, 610–623.

Biggs, L.C., and Mikkola, M.L. (2014). Early inductive events in ectodermal appendage morphogenesis. Semin. Cell Dev. Biol. *25-26*, 11–21.

Blanpain, C., Lowry, W.E., Geoghegan, A., Polak, L., and Fuchs, E. (2004). Self-renewal, multipotency, and the existence of two cell populations within an epithelial stem cell niche. Cell *118*, 635–648.

Botchkarev, V.A., and Sharov, A.A. (2004). BMP signaling in the control of skin development and hair follicle growth. Differentiation *72*, 512–526.

Botchkarev, V.A., Botchkareva, N.V., Roth, W., Nakamura, M., Chen, L.H., Herzog, W., Lindner, G., McMahon, J.A., Peters, C., Lauster, R., et al. (1999). Noggin is a mesenchymally derived stimulator of hair-follicle induction. Nat. Cell Biol. *1*, 158–164.

Chen, D., Jarrell, A., Guo, C., Lang, R., and Atit, R. (2012). Dermal β-catenin activity in response to epidermal Wnt ligands is required for fibroblast proliferation and hair follicle initiation. Development *139*, 1522–1533.

Chen, E.Y., Tan, C.M., Kou, Y., Duan, Q., Wang, Z., Meirelles, G.V., Clark, N.R., and Ma'ayan, A. (2013). Enrichr: interactive and collaborative HTML5 gene list enrichment analysis tool. BMC Bioinformatics *14*, 128.

Chiang, C., Swan, R.Z., Grachtchouk, M., Bolinger, M., Litingtung, Y., Robertson, E.K., Cooper, M.K., Gaffield, W., Westphal, H., Beachy, P.A., and Dlugosz, A.A. (1999). Essential role for Sonic hedgehog during hair follicle morphogenesis. Dev. Biol. *205*, 1–9.

Clavel, C., Grisanti, L., Zemla, R., Rezza, A., Barros, R., Sennett, R., Mazloom, A.R., Chung, C.-Y., Cai, X., Cai, C.-L., et al. (2012). Sox2 in the dermal papilla niche controls hair growth by fine-tuning BMP signaling in differentiating hair shaft progenitors. Dev. Cell *23*, 981–994.

Colombo, S., Champeval, D., Rambow, F., and Larue, L. (2012). Transcriptomic analysis of mouse embryonic skin cells reveals previously unreported genes expressed in melanoblasts. J. Invest. Dermatol. *132*, 170–178.

Driskell, R.R., Giangreco, A., Jensen, K.B., Mulder, K.W., and Watt, F.M. (2009). Sox2-positive dermal papilla cells specify hair follicle type in mammalian epidermis. Development *136*, 2815–2823.

Driskell, R.R., Lichtenberger, B.M., Hoste, E., Kretzschmar, K., Simons, B.D., Charalambous, M., Ferron, S.R., Herault, Y., Pavlovic, G., Ferguson-Smith, A.C., and Watt, F.M. (2013). Distinct fibroblast lineages determine dermal architecture in skin development and repair. Nature *504*, 277–281.

Ellis, P., Fagan, B.M., Magness, S.T., Hutton, S., Taranova, O., Hayashi, S., McMahon, A., Rao, M., and Pevny, L. (2004). SOX2, a persistent marker for multipotential neural stem cells derived from embryonic stem cells, the embryo or the adult. Dev. Neurosci. *26*, 148–165.

Fetting, J.L., Guay, J.A., Karolak, M.J., Iozzo, R.V., Adams, D.C., Maridas, D.E., Brown, A.C., and Oxburgh, L. (2013). FOXD1 promotes nephron progenitor differentiation by repressing decorin in the embryonic kidney. Development *141*, 17–27.

Greco, V., Chen, T., Rendl, M., Schober, M., Pasolli, H.A., Stokes, N., Dela Cruz-Racelis, J., and Fuchs, E. (2009). A two-step mechanism for stem cell activation during hair regeneration. Cell Stem Cell *4*, 155–169.

Grisanti, L., Clavel, C., Cai, X., Rezza, A., Tsai, S.-Y., Sennett, R., Mumau, M., Cai, C.-L., and Rendl, M. (2013a). Tbx18 targets dermal condensates for labeling, isolation, and gene ablation during embryonic hair follicle formation. J. Invest. Dermatol. *133*, 344–353.

Grisanti, L., Rezza, A., Clavel, C., Sennett, R., and Rendl, M. (2013b). Enpp2/Autotaxin in dermal papilla precursors is dispensable for hair follicle morphogenesis. J. Invest. Dermatol. *133*, 2332–2339.

Hiremath, M., Dann, P., Fischer, J., Butterworth, D., Boras-Granic, K., Hens, J., Van Houten, J., Shi, W., and Wysolmerski, J. (2012). Parathyroid hormone-related protein activates Wnt signaling to specify the embryonic mammary mesenchyme. Development *139*, 4239–4249.

Hsu, Y.-C., Pasolli, H.A., and Fuchs, E. (2011). Dynamics between stem cells, niche, and progeny in the hair follicle. Cell *144*, 92–105.

Huh, S.-H., Närhi, K., Lindfors, P.H., Häärä, O., Yang, L., Ornitz, D.M., and Mikkola, M.L. (2013). Fgf20 governs formation of primary and secondary dermal condensations in developing hair follicles. Genes Dev. *27*, 450–458.

Jamora, C., DasGupta, R., Kocieniewski, P., and Fuchs, E. (2003). Links between signal transduction, transcription and adhesion in epithelial bud development. Nature *422*, 317–322.

Jessen, K.R., and Mirsky, R. (2005). The origin and development of glial cells in peripheral nerves. Nat. Rev. Neurosci. *6*, 671–682.

Jonsson, M., Björntorp Mark, E., Brantsing, C., Brandner, J.M., Lindahl, A., and Asp, J. (2004). Hash4, a novel human achaete-scute homologue found in fetal skin. Genomics *84*, 859–866.

Kanehisa, M., and Goto, S. (2000). KEGG: Kyoto encyclopedia of genes and genomes. Nucleic Acids Res. *28*, 27–30.

Kanehisa, M., Goto, S., Sato, Y., Kawashima, M., Furumichi, M., and Tanabe, M. (2014). Data, information, knowledge and principle: back to metabolism in KEGG. Nucleic Acids Res. *42*, D199–D205.

Kiso, M., Tanaka, S., Saba, R., Matsuda, S., Shimizu, A., Ohyama, M., Okano, H.J., Shiroishi, T., Okano, H., and Saga, Y. (2009). The disruption of Sox21-mediated hair shaft cuticle differentiation causes cyclic alopecia in mice. Proc. Natl. Acad. Sci. USA *106*, 9292–9297.

Laurikkala, J., Pispa, J., Jung, H.-S., Nieminen, P., Mikkola, M., Wang, X., Saarialho-Kere, U., Galceran, J., Grosschedl, R., and Thesleff, I. (2002). Regulation of hair follicle development by the TNF signal ectodysplasin and its receptor Edar. Development *129*, 2541–2553.

Lee, J., and Tumbar, T. (2012). Hairy tale of signaling in hair follicle development and cycling. Semin. Cell Dev. Biol. *23*, 906–916.

Levy, V., Lindon, C., Harfe, B.D., and Morgan, B.A. (2005). Distinct stem cell populations regenerate the follicle and interfollicular epidermis. Dev. Cell *9*, 855–861.

Lien, W.-H., Guo, X., Polak, L., Lawton, L.N., Young, R.A., Zheng, D., and Fuchs, E. (2011). Genome-wide maps of histone modifications unwind in vivo chromatin states of the hair follicle lineage. Cell Stem Cell *9*, 219–232.

Millar, S.E. (2002). Molecular mechanisms regulating hair follicle development. J. Invest. Dermatol. *118*, 216–225.

Morris, R.J., Liu, Y., Marles, L., Yang, Z., Trempus, C., Li, S., Lin, J.S., Sawicki, J.A., and Cotsarelis, G. (2004). Capturing and profiling adult hair follicle stem cells. Nat. Biotechnol. *22*, 411–417.

Philbrick, W.M., Dreyer, B.E., Nakchbandi, I.A., and Karaplis, A.C. (1998). Parathyroid hormone-related protein is required for tooth eruption. Proc. Natl. Acad. Sci. USA *95*, 11846–11851.

Reddy, S., Andl, T., Bagasra, A., Lu, M.M., Epstein, D.J., Morrisey, E.E., and Millar, S.E. (2001). Characterization of Wnt gene expression in developing and postnatal hair follicles and identification of Wnt5a as a target of Sonic hedgehog in hair follicle morphogenesis. Mech. Dev. *107*, 69–82.

Rendl, M., Lewis, L., and Fuchs, E. (2005). Molecular dissection of mesenchymal-epithelial interactions in the hair follicle. PLoS Biol. *3*, e331.

Rezza, A., Sennett, R., and Rendl, M. (2014). Adult stem cell niches: cellular and molecular components. Curr. Top. Dev. Biol. *107*, 333–372.

Rezza, A., Sennett, R., Tanguy, M., Clavel, C., and Rendl, M. (2015). PDGF signalling in the dermis and in dermal condensates is dispensable for hair follicle induction and formation. Exp. Dermatol. *24*, 468–470.

Rhee, H., Polak, L., and Fuchs, E. (2006). Lhx2 maintains stem cell character in hair follicles. Science *312*, 1946–1949.

Schneider, M.R., Schmidt-Ullrich, R., and Paus, R. (2009). The hair follicle as a dynamic miniorgan. Curr. Biol. *19*, R132–R142.

Sennett, R., and Rendl, M. (2012). Mesenchymal-epithelial interactions during hair follicle morphogenesis and cycling. Semin. Cell Dev. Biol. *23*, 917–927.

Sennett, R., Rezza, A., Dauber, K.L., Clavel, C., and Rendl, M. (2014). Cxcr4 is transiently expressed in both epithelial and mesenchymal compartments of nascent hair follicles but is not required for follicle formation. Exp. Dermatol. *23*, 748–750.

St-Jacques, B., Dassule, H.R., Karavanova, I., Botchkarev, V.A., Li, J., Danielian, P.S., McMahon, J.A., Lewis, P.M., Paus, R., and McMahon, A.P. (1998). Sonic hedgehog signaling is essential for hair development. Curr. Biol. *8*, 1058–1068.

Suzuki, K., Yamanishi, K., Mori, O., Kamikawa, M., Andersen, B., Kato, S., Toyoda, T., and Yamada, G. (2000). Defective terminal differentiation and hypoplasia of the epidermis in mice lacking the Fgf10 gene. FEBS Lett. *481*, 53–56.

Tsai, S.-Y., Clavel, C., Kim, S., Ang, Y.-S., Grisanti, L., Lee, D.-F., Kelley, K., and Rendl, M. (2010). Oct4 and klf4 reprogram dermal papilla cells into induced pluripotent stem cells. Stem Cells *28*, 221–228.

Tsai, S.-Y., Sennett, R., Rezza, A., Clavel, C., Grisanti, L., Zemla, R., Najam, S., and Rendl, M. (2014). Wnt/β-catenin signaling in dermal condensates is required for hair follicle formation. Dev. Biol. *385*, 179–188.

Tumbar, T., Guasch, G., Greco, V., Blanpain, C., Lowry, W.E., Rendl, M., and Fuchs, E. (2004). Defining the epithelial stem cell niche in skin. Science *303*, 359–363.

Wang, X., and Wu, Y. (2014). Molecular signals underlying hair follicle morphogenesis and cutaneous regeneration. In Tumor Dormancy, Quiescence, and Senescence, *Volume 2*, M.A. Hayat, ed. (Dordrecht, the Netherlands: Springer Netherlands), pp. 89–100.

Woodhoo, A., and Sommer, L. (2008). Development of the Schwann cell lineage: from the neural crest to the myelinated nerve. Glia *56*, 1481–1490.

Zhang, Y., Tomann, P., Andl, T., Gallant, N.M., Huelsken, J., Jerchow, B., Birchmeier, W., Paus, R., Piccolo, S., Mikkola, M.L., et al. (2009). Reciprocal requirements for EDA/EDAR/NF-kappaB and Wnt/beta-catenin signaling pathways in hair follicle induction. Dev. Cell *17*, 49–61.